

A Novel Skeleton-Based Human Activity Discovery Using Particle Swarm Optimization with Gaussian Mutation

Parham Hadikhani*, Daphne Teck Ching Lai, and Wee-Hong Ong

Abstract—Human activity discovery aims to cluster the activities performed by humans, without any prior information of what defines each activity. Most methods presented in human activity recognition are supervised, where there are labeled inputs to train the system. In reality, it is difficult to label activities data because of its huge volume and the variety of activities performed by humans. In this paper, an unsupervised approach is proposed to perform human activity discovery in 3D skeleton sequences. First, important frames are selected based on kinetic energy. Next, the displacement of joints, statistical displacements, angles, and orientation features are extracted to represent the activities information. Since not all extracted features have useful information, the dimension of features is reduced using PCA. Most human activity discovery proposed are not fully unsupervised. They use pre-segmented videos before categorizing activities. To deal with this, we have used sliding time window to segment the time series of activities with some overlapping. Then, activities are discovered by a hybrid particle swarm optimization with Gaussian mutation algorithm to provide diverse solutions. Finally, k-means is applied to the outcome centroids from each iteration of the PSO to overcome the slow convergence rate of PSO. Experiments on three datasets have been presented and the results show the proposed method has superior performance in discovering activities in compared to the other state-of-the-art methods and has increased accuracy of at least 4% on average.

Index Terms—Human activity discovery, Unsupervised learning, Clustering, Feature extraction, Dimension reduction, Skeleton sequence, Particle swarm optimization

I. INTRODUCTION

HUMAN Activity Recognition (HAR) has attracted much attention due to its applications in fields such as human-computer interaction, intelligent transportation systems, and monitoring applications [1]. Activity recognition aims to identify actions and activities that humans perform in different environments automatically. The input to a vision-based HAR system is a sequence of frames of a person performing different movements. The output is a set of labels representing the actions taken or activities in those movements. Many existing works use visual data as input. But such data have considerable complexity detrimental to the performance of HAR systems. These complexities include cluttered background, changes in brightness and points of view. Using 3D skeleton data partially overcome these complexities and protect people’s privacy when RGB data is not captured. Each frame represented by

3D coordinates of the main body joints is appropriate for representing human actions [2] and can be easily obtained in real-time with low-cost depth sensors [3].

As shown in Fig. 1, there are at least seven steps in vision-based HAR systems. Vision sensors capture activities performed by a person. The skeletal information comprising of joints coordinates are extracted from captured videos, containing image sequences called frames. Meaningful features are then extracted for more accurate activity discovery. The system without using manual annotations and having any guidance for activities discovers them by clustering the most similarity activities from a set of different activities. In other word, the system try to differentiate observed activities based on the likeness of extracted features. The discovered activity clusters are used in the learning process to model each cluster of activity and recognize future activities.

Significant progress has been made in the supervised learning of activity models [4], illustrated in blocks (f) and (g) of Fig. 1. The learning and recognition steps rely on human-labeled training data to categorize activities if activity discovery (block e) was not performed. Human activity discovery is a part of the HAR process where activities are categorized based on their similarities without any knowledge of activity labels or any information that characterizes an activity, making this step particularly challenging. In other words, activity discovery is like a child learning. There is no prior information to define a specific sequence of movements to mean a particular activity such as crawling or waving and so forth to the child learner. Using the ability to differentiate, they learn from unlabeled data and form a model that can post-label new data based on that training. In human activity discovery, there is no known information or knowledge about a particular movement, including its start to end, for example when someone is picking up something. This means the input is a series of movements where there is no knowledge of the start and endpoints to indicate each activity. In some existing work, the input data have been segmented by activity [2]. Thus, the start and endpoints of the activities are already known, although the method of grouping activities may be unsupervised.

In this paper, we focus on the less developed activity discovery comprising the block (d) to (e) of Fig. 1 by developing an effective methodology to extract good features and clusters activities without any label. Keyframe selection [5] and PCA are used to remove redundant frames and features to reduce time complexity and increase accuracy. A feature extraction methodology is applied to extract features from the most

P. Hadikhani, D.T.C. Lai, and W.H. Ong are with the School of Digital Science, Universiti Brunei Darussalam, Brunei. E-mail: {20h8561, daphne.lai, weehong.ong}@ubd.edu.bn.

D.T.C. Lai, and W.H. Ong are with Institute of Applied Data Analytics, Universiti Brunei Darussalam, Brunei

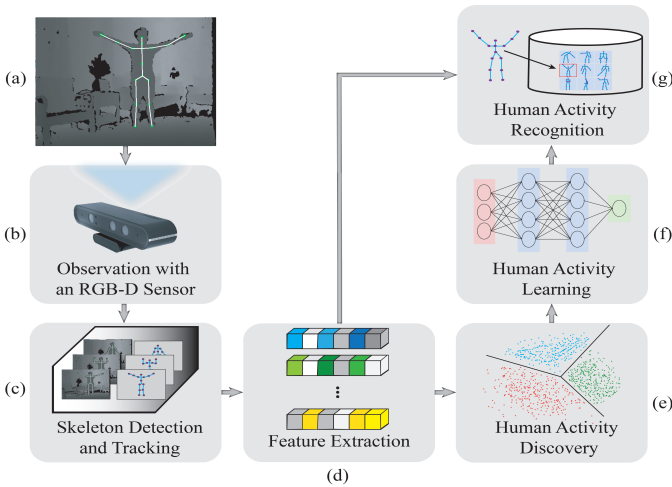


Fig. 1: Overview of HAR system: (a) performed activities are (b) captured by a Kinect sensor. (c) After that, pose of humans are estimated by extracting joints. (d) To make raw data more usable, their salient and defining features are identified. (e) Based on the similarities and differences, activities are discovered. (f) Afterwards, the system begins to learn from the discovered activities and (g) finally human activities are recognized.

informative joints and bones, including joint displacement, joint orientation, and statistical time domain. As our first study, a hybrid Particle Swarm Optimization (PSO) clustering technique, requiring a known a priori of cluster number is proposed to find activities. Sometimes particles converge to a specific point between the best global and personal positions and get trapped in local optima. This difficulty arises when the swarm's variety reduces and the swarm is unable to escape from a local optimum [6]. To address this, a hybrid PSO with Gaussian mutation is proposed to promote diversity to avoid early convergence. Then, K-means is applied to the centroids obtained by PSO to refine their location and get the best possible solution. Our methodology performs activity discovery using unsegmented input data and the proposed techniques used are unsupervised with no prior knowledge of the labels of the different activities. The main contributions of this paper are:

- A methodology consists of keyframe selection, feature extraction, and PCA to represent human activities.
- A hybrid PSO algorithm to discover and group unlabelled of human activities observations into individual activity classes. PSO is customized by applying the Gaussian mutation, which is based on the advantages of two methods [7] and [8], on the global best's centroids to increase the diversity of selected clusters in the global best.
- Integrating K-means to refine the obtained cluster centers from the PSO to improve the exploitation of the algorithm.
- An evaluation of the performance of the proposed methodology comparing with existing, latest fully unsupervised methodology for HAR. We did not compare

those of deep learning techniques as they are supervised techniques.

In this paper, the background and related methods are discussed in section II. The methodology is described in section III. We present the evaluation of the proposed approach, comparing with state-of-the-art (SOTA) techniques in Section IV, and finally, the conclusion is stated in Section V.

II. RELATED WORKS

Feature extraction from 3D skeletal human activities data. Skeletal data includes the number of joints, and each joint contains three-dimensional coordinates. Since motion of the joints have essential information for any activity, feature extraction is vital. There are various methods for representation of the motion of skeletal joints such as calculating the difference between the joints in the same frame and same joints in different frames [9], using Histogram Oriented of Joints [10], Dynamic Time Warping algorithm [11], Covariance of 3D Joints [12], generating joint rotation matrix concerning the person's torso [13], and extracting the angles and orientations of the most informative body joints [14]. However, most of these methods extract one aspect of the skeletal data features that leads to other important aspects of activities being overlooked. As a result, there is a decrease in accuracy in the final result because of the insufficient discriminating ability of the extracted features. Moreover, due to the complexity of feature calculations, some of these methods cause computational latency. The difference between our paper with previous works for extracting features is that We have combined the feature extraction techniques from [9], [15], [14] to extract three skeletal features from informative joints and keyframes. Previously, these features have been applied separately and most of them have used all of the joints and frames that increases additional information. This increases the time complexity and also reduces the performance of identifying the activities. There are some methods like [5] and [16] that have tried to select some frames that are more distinguishing compared to other frames and remove redundant information with the assistance of kinetic energy. However, these methods are applied to each activity sample separately. In other words, in [5] and [16], keyframes were selected in a supervised manner. In contrast, we apply the above methods in our proposed method to select keyframes without knowing the beginning and end of the activities.

Recognition and discovery of 3D skeletal human activity. Many studies in HAR used supervised approaches [17], [18], [19]. Yadav et al. [20] combined long-short term memory networks and convolutional neural networks for recognizing human activity and fall detection. They used some handcrafted features, including geometrical and kinematic features to guide their proposed model. Zhang et al. [21] proposed an end-to-end semantics-guided neural networks framework. They provided two semantic forms based on joints and frames and used GCN and CNN layers to find the dependence of joints and frames, respectively. Si et al. [22] proposed a novel model based on a recurrent network. They applied graph convolutional layer into the LSTM network to improve

the performance of traditional LSTM. They also introduced an attention gate inside the LSTM to capture discriminative features. Xia et al. [23] provided a graph convolution network based on spatial and temporal. They applied attention layer on the model to generate discriminative features and modified feature maps. Then, a softmax classifier was used to categorize the activities. Cai et al. [24] introduced a scheme to capture visual information surrounding each skeleton joint and achieve local motion cues. They extracted features from both skeleton and RGB data by using two graph convolutional networks. Then, concatenated both type of features were concatenated and activities were classified by calculating a score based on linear blending. The problem with these approaches is that they require activity labels in the training data. The labels were annotated by humans during data preparation. It makes these methods impractical with real-life data that are mainly unlabeled. In our work, we do not use labels for training in our algorithm. The algorithm discovers activities by looking for similar features between them. In addition, the methods mentioned above use deep learning techniques, while as a first study, we do not use them in our method and the focus is on developing a comprehensive model for HAD as a baseline.

There are several approaches that try to address the HAR in an unsupervised way. Wang et al. [25] presented a deep clustering method based on a dual-stack auto-encoder to map raw data to spatio-temporal features. After extracting features, the radial basis function neural network was used to classify the activities. Su et al. [4] provided an unsupervised model by employing a bi-directional recurrent neural network and used K-NN to classify the activities. Liu et al. [26] designed a spatial-temporal asynchronous normalization method to reduce redundant information related to the time and normalize the spatial features. Next, they used gated recurrent unit auto-encoder to feature vector. First, all of these methods received the activities already segmented which has enabled them to be aware of the differences between the activities before performing the recognition. Second, in most of these methods, only feature extraction was performed without supervision. For the rest of the operations, supervised classification method was used to learn activity models using activity labels.

On the other hand, human activity discovery can automatically categorize human activity in a fully unsupervised way and the challenge is learning from unlabeled data. The majority of existing methods were developed for sensor-based [27], [28] and RGB video data [29], [30]. The challenges of sensor-based approach are difficult to implement in the environment and take a long time to install [31]. Furthermore, it is impractical for people to wear sensors everywhere. With RGB videos, the problems faced are millions of pixel values, illumination variations, viewpoint changes, and cluttered backgrounds [3]. In this work, we concentrate on 3D skeleton-based data as it does not have the problems of the other two data types. One of the first work in HAD was performed by Ong et al. [31]. They proposed an autonomous learning technique based on the mixture of Gaussian hidden Markov model. To discover the activities, they introduced an incremental clustering approach based on k-means to deal with the undefined number of clusters. An issue with their approach is that they have used

k-means to discover the activities that get stuck into the local optimum easily and they have not examined all aspects of the skeleton data features. Moreover, they extracted all the features from all joints, resulting in more redundant data and increased discovery error. Recently several approaches have been proposed by [2] to solve HAR without labels. In their proposed methods, several clustering methods, including spectral clustering (SC), elastic net subspace clustering (ENSC), and sparse subspace clustering (SSC) were used, which used covariance descriptors. They used an affinity matrix to find similarities and then applied spectral clustering. In addition, a time stamp pruning approach was used to remove redundant data to normalize temporal features. Although they have achieved impressive results, the data used were already segmented by activity before performing discovery. It means that the activities are already categorized. Because each sample contains an activity that performs completely. In other words, the beginning and end of each the activity is clear.

In this paper, we propose an approach to discover activities from untrimmed videos without knowing the label of activities. It makes this method suitable for use in real-world scenarios. In addition, we use a feature extraction approach to examine most aspects of skeleton data along with a keyframe selector to reduce redundant information and discovery accuracy.

III. PROPOSED HUMAN ACTIVITY DISCOVERY

In this section, the proposed method is presented, as shown in Fig. 2. Keyframes are first extracted from input video based on the kinetic energy of all frames. Three types of features including spatial and temporal displacement, mean and standard deviation differences, and orientation and angle features are extracted. Next, feature vectors are reduced by PCA and frames are sampled in specific periods to segment the activity stream. Finally, the proposed clustering technique assigns each sample to an appropriate category of activities. The details of each part of the methodology are described below.

A. Keyframe selection

Keyframe selection is a process to select frames reflecting the main activities in the video. There are some method like [5] and [16] that have tried to select some frames that are more distinguishing compared to other frames. However, these methods were applied to each activity sample separately. In other words, in methods [5] and [16], keyframes were selected in a supervised manner. In our proposed method, keyframes are selected without knowing the beginning and end of the activities. To find the keyframes, the kinetic energy $E(f_i)$ of each frame f_i is calculated [5] using Eq.(1), based on the displacement of joints over time. In this way, the movement of a joint j between frame i and $i-1$ is calculated for all joints (J). The sum of the movements for all joints is the energy of the current frame. Frames with local maxima and minima amount of kinetic energy compared to neighboring frames are considered as keyframes (see Fig. 3) Because these are the

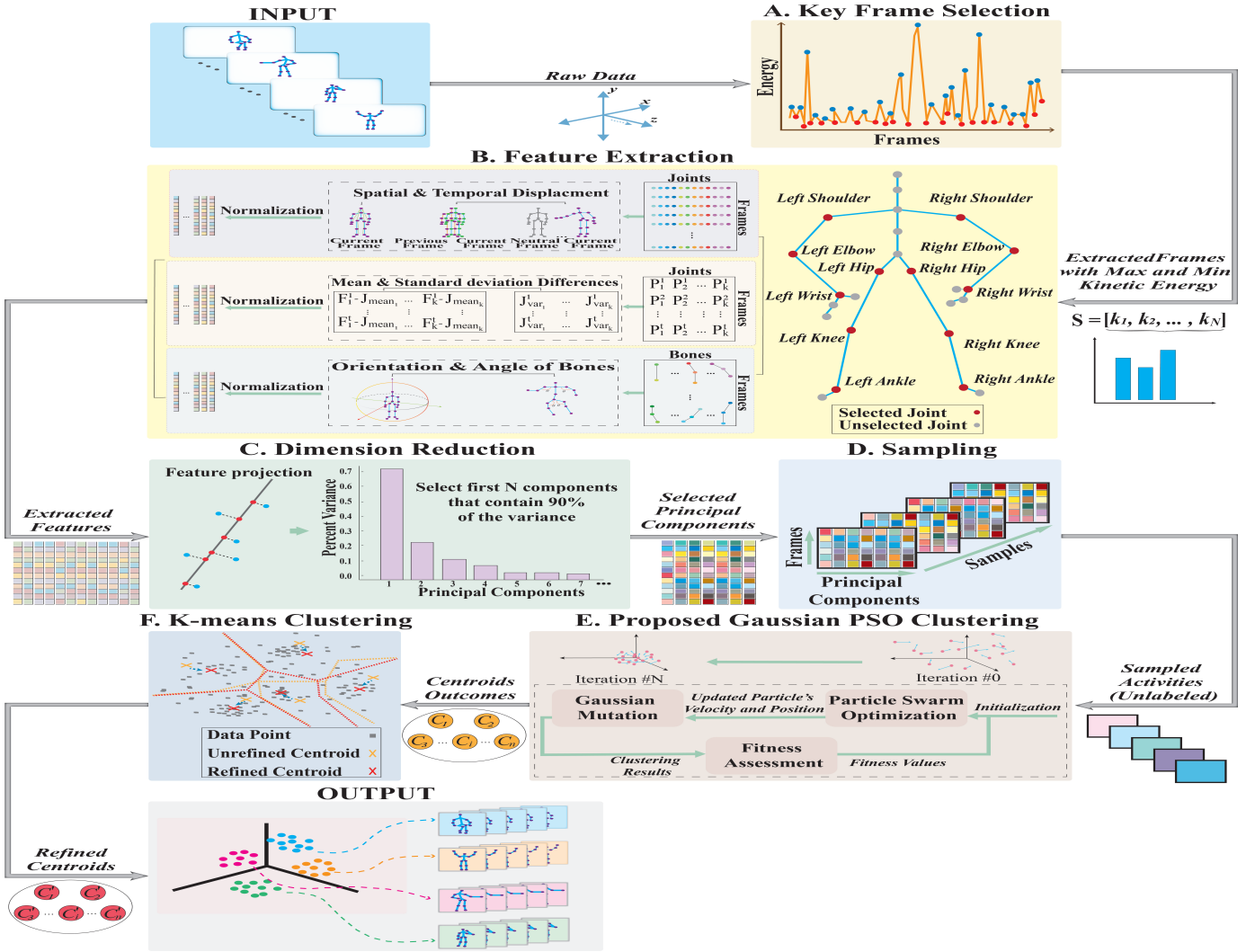


Fig. 2: Methodology of the proposed approach: First, (A) keyframes are selected from the video sequence by computing kinetic energy. Then, (B) features based on different aspects of skeleton including displacement, orientation, and statistical are extracted. (C) Principal components are then chosen by applying PCA on the features. Next, (D) overlapping time windows is used to segment a series of keyframes as activity samples. (E) Hybrid PSO clustering with Gaussian mutation operator is used to discover the groups of activities. (F) Eventually, K-means clustering is applied to the resultant cluster centers to refine the centroids.

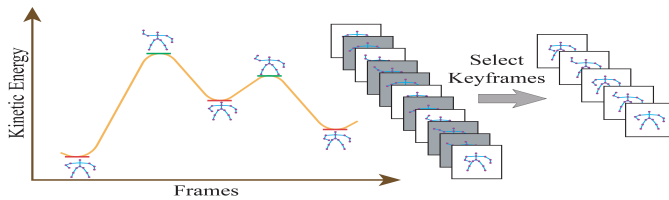


Fig. 3: Illustration of the keyframe selection.

energy's extreme points, which are meant to resemble crucial posture data.

$$E(f_i) = \sum_{j=1}^J E(f_i^j) = 1/2 \sum_{j=1}^J (f_i^j - f_{i-1}^j)^2 \quad (1)$$

B. Feature extraction

To represent the activities, a set of statistical displacements, angles and orientation features for encoding key aspects of activities are extracted. These important features are extracted from selected (informative) joints in the data to describe the shape and movement of human. Selected joints have been obtained based on experimental tests that included left and right hand, foot, hip, shoulder, elbow and knee. These joints have more movement and contribution than other joints such as torso in activities. We use information related to the position and movement of joints, the orientation and angle between a pair of bones and activity variation over time. The normalization procedure [9] is performed on all features.

1) *Displacement features:* Joint displacement-based features encode information on the position and motion of body

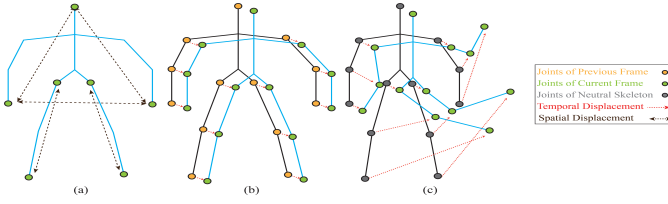


Fig. 4: (a) Spatial displacement of pairwise joints in the same frame. Temporal displacement of current frame from (b) previous frame and (c) the neutral frame

joints, particularly displacement between joints of a pose and position differences of skeleton joints across time [9].

- Spatial joint displacement is computed using pairwise Euclidean distances between joints P_i and P_j ($i \neq j$) in 3D space in the same frame, Eq.(2). The joint pairs used are both hands, hands and head, and hip and feet at both sides, giving 5 features per frame, (see Fig. 4(a)).

$$PairwiseDistances = \sqrt{\sum_{x,y,z} (P_i - P_j)^2} \quad (2)$$

- Temporal joint displacement is calculated based on two modes. T_{cp} is the difference between each selected joint P_i in current frame P_i^c and previous frame P_i^{c-1} (see Fig. 4(b)) to determine the small changes in joint movement over time (Eq.(3)). T_{cn} is the difference between each selected joint of current frame and the frame of neutral pose (We randomly select a standing position as a neutral position) P_i^n , illustrated in Fig. 4(c), to find general changes in joint movements as given in Eq.(4).

$$T_{cp} = P_i^c - P_i^{c-1} \quad (3)$$

$$T_{cn} = P_i^c - P_i^n \quad (4)$$

2) *Statistical features*: The mean and standard deviation of time-domain features express how activity changes over time, particularly in distinguishing between activities related to the arms and legs. Thus, statistical time-domain features encode variations across a collection of poses of an activity in time-domain. These features are calculated by the difference of selected joint P_i^c in current frame from mean $P_{(i,mean)}$ and standard deviation $P_{(i,std)}$ of the selected joint coordinates within an activity sequence as given by Eq.(5) and (6) [9].

- Joint coordinate-mean difference

$$P_{i(mean)}^c = P_i^c - P_{(i,mean)}, P_{(i,mean)} = \frac{1}{N} \sum_{c=1}^N P_i^c \quad (5)$$

N is the number of frames.

- Joint coordinate-standard deviation difference

$$P_{(i,std)}^c = P_i^c - \sqrt{\frac{\sum_{i=c}^N (P_i^c - P_{(i,mean)})^2}{N}} \quad (6)$$

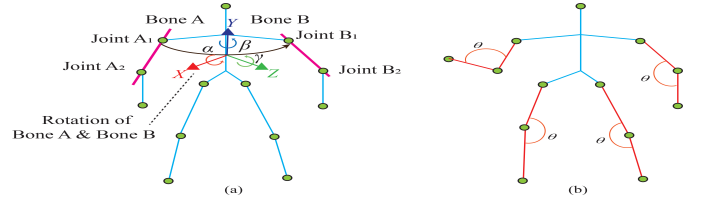


Fig. 5: (a) Illustration of the rotation between two bones A and B. α , β , and γ are the orientation of angles. (b) The angles of the selected body bones. The angles of elbow-wrist and shoulder-elbow at both sides and angles between the bones of hip-knee and knee-ankle at both sides are used to calculate angle features.

3) *Orientation features*: The three-dimensional coordinate system $\{x,y,z \in R^3\}$ represents points as joints. x , y , and z denote the 3D coordinates of joints. Joints and bones can be described by the orthonormal vectors [15] as follow:

$$P_i^f = x_i^f e_1 + y_i^f e_2 + z_i^f e_3 \quad (7)$$

$$B_{ij}^f = (x_i^f - x_j^f) e_1 + (y_i^f - y_j^f) e_2 + (z_i^f - z_j^f) e_3 \quad (8)$$

where P_i^f is the i th skeleton joint in the f th frame and e_1, e_2, e_3 are orthonormal vectors. B_{ij}^f is the bone between two adjacent joints P_i^f and P_j^f . Moreover, magnitude and direction of two bones a and b are represented by geometric product. Where this product is the sum of internal ($a \cdot b$) and external ($a \wedge b$) product. Where the inner product is used to compute the length and angle between two bones a and b . The outer product of two bones can be regarded as an oriented plane containing a and b . The orientation and angles between bones features are obtained in the process described as follows.

- The rotation matrix is a transformation matrix that describes the rotation from a bone to another. Three angles are required to define the rotation matrix between two bones. The rotation angles are considered as orientation features. The elements of these features are the rotation of bones relative to the x , y , and z axes (see Fig. 5(a)).
- The angle features consist of the angles between the bones of elbow-wrist and shoulder-elbow at both sides and the angles between the bones of hip-knee and knee-ankle at both sides. These angles are highlighted in Fig. 5(b) and calculated as below:

$$\theta = 180 \times \frac{\arctan^2\left(\frac{\|bone_i \wedge bone_j\|}{\|bone_i \cdot bone_j\|}\right)}{\pi} + 180 \quad (9)$$

where $bone_i$ and $bone_j$ are determined by Eq.(8)

C. Feature selection and sampling

For fast clustering and complexity reduction, key features are extracted by PCA. Then, sliding windows are used to segment frames into time windows. Each window comprises of 15 frames. The overlap of sliding windows increases performance. Because it increases the number of samples and avoid pruning important events like transition between activities [32]. The first 15 frames do not overlap while in other samples, their first frame starts from the last frame of the previous sample (see Fig. 6).

D. Proposed clustering

PSO is a population-based optimization algorithm [33]. A population is made up of a number of particles and each particle represents a solution and moves according to its speed. The changes in velocity and position of the particles are calculated based on the following formula:

$$x_i(t+1) = x_i(t) + v_i(t) \quad (10)$$

$$v_i(t+1) = w \times v_i(t) + c_1 \times rand_1 \times (pbest_i(t) - x_i(t)) + c_2 \times rand_2 \times (gbest(t) - x_i(t)) \quad (11)$$

$$w = \frac{w_{max} + t \times (w_{max} - w_{min})}{t_{max}} \quad (12)$$

$$c_1(t+1) = (c_{1_{max}} - c_{1_{min}}) \times \frac{t}{t_{max}} + c_{1_{max}} \quad (13)$$

$$c_2(t+1) = (c_{2_{max}} - c_{2_{min}}) \times \frac{t}{t_{max}} + c_{2_{max}} \quad (14)$$

In Eq.(10) and (11) $x_i(t)$ and $v_i(t)$ are the position and velocity of the particle i at time t respectively. $pbest_i$ is the best position found by the particle i . $gbest$ is the best position found in the population. w is the inertial weight defined by Eq.(12) and starts to decrease from w_{max} . c_1 and c_2 are acceleration coefficients expressed by Eq.(13) and (14). The $c_{1_{max}}$, $c_{2_{max}}$ and $c_{1_{min}}$, $c_{2_{min}}$ are initial and final values, respectively, t is the number of iterations and t_{max} is the maximum number of iterations [34]. $rand_1$ and $rand_2$ are random variables between 0 and 1. Each solution is evaluated by Eq.(15) which should be minimized to achieve proper clustering.

$$SSE = \sum_{k=1}^K \sum_{\forall x \in C_k} \|x_i - \mu_k\|^2 \quad (15)$$

x_i is a data point belonging to the cluster C_k and μ_k is the mean of the cluster C_k . k is the number of clusters specified. To avoid in local optimum, a Gaussian mutation operator based on [7] and [8] is applied to the global particle as follows:

$$v'_{gbest}(d) = v_{gbest}(d) \times G(0, h) \times (x_{max}(d) - x_{min}(d)) \quad (16)$$

$$x'_{gbest}(d) = x_{gbest}(d) + G(0, h) \times v'_{gbest}(d) \quad (17)$$

Where x_{gbest} and v_{gbest} represent the position and velocity of global best particle. x_{max} and x_{min} are the maximum and minimum value in d^{th} dimension. Gaussian $(0, h)$ is Gaussian distribution with the mean 0 and the variance h . h is linearly decreased during each iteration according to Eq.(18) to ensure that the capability of exploration is strong initially and, exploitation is strong at the later stage.

$$h(t+1) = h(t) - (1/t_{max}) \quad (18)$$

Where t_{max} is the maximum number of iterations. Fig. 7 is an illustration of the Gaussian mutation.

The velocity of the particles reduces quickly as PSO approaches the global optimum, and in most circumstances, the most ideal solution is not achieved. For this reason, K-means is

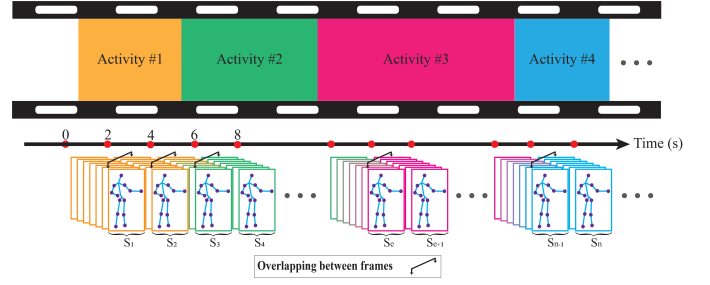


Fig. 6: Illustration of sampling based on overlapping sliding windows. Each sample (S_1, S_2, \dots, S_n), except the first sample, starts with the last frame of the previous sample.

applied to the obtained centroids from PSO to refine the them. The routine of the proposed clustering algorithm is shown in Algorithm 1.

Algorithm 1: Hybrid PSO with Gaussian Mutation and K-means (HPGMK)

Input: $D = \{d_1, d_2, \dots, d_n\}$ //Set of data points
 k //Number of desired activities (clusters)

Output: Set of k clusters

- 1 Initialize a population of particles with random positions and velocities in the search space
 - 2 **for** $t=1$ to the maximum number of iteration **do**
 - 3 **for** each particle i **do**
 - 4 Update position and velocity of particle i according to Eq.(10) and Eq.(11)
 - 5 Evaluate fitness value of particle i according to the fitness function in Eq.(15)
 - 6 Update $pbest_i(t)$ and $gbest(t)$ if necessary
 - 7 **for** T times **do**
 - 8 Mutate $gbest(t)$ according to Eq.(16) and (17)
 - 9 Compare mutated $gbest(t)$ with previous and choose the best as new $gbest(t)$
 - 10 Use $gbest(t)$ as the initial centroids
 - 11 **while** until no change **do**
 - 12 // Refining the centroids
 - 13 Calculate distances of data points to centroids
 - 14 Assign data points to the closest cluster
 - 14 Centroids are updated using the following equation

$$centroid_i = \frac{1}{n_i} \sum_{\forall d_i \in C_i} d_i,$$
 - 15 where n_i is the number of data points in the cluster i
-

IV. EXPERIMENTS

A. Datasets

Five datasets were used to evaluate the effectiveness of proposed method: Cornell Activity Dataset (CAD-60) [13], UTKinect-Action3D (UTK) [10], Florence3D (F3D) [35], Kinect Activity Recognition Dataset (KARD) [19], and MSR

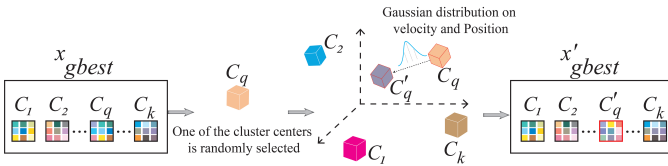


Fig. 7: Visualization of the Gaussian Mutation Operator. In each iteration of hybrid PSO, one centroid (C_q) is chosen from x_{gbest} randomly. Then, Gaussian distribution is applied on position and velocity of the selected centroid based on Eq.(16) and (17) to create a new offspring C'_q . The new global best (x'_{gbest}) is then compared to x_{gbest} . If x'_{gbest} has better fitness value than x_{gbest} , x'_{gbest} is replaced with new global best.

DailyActivity3D (MSR) [36]. These datasets have different dimensions, features, and activities. Table I shows the statistical information of these datasets. They are discussed as follows.

TABLE I: Number of activities, subjects and videos in the five datasets used

Dataset	CAD-60	UTK	F3D	KARD	MSR
Activities	14	10	9	18	16
Subjects	4	10	10	10	10
Videos	60	200	215	2160	320

CAD-60: This dataset includes 14 activities: *rinsing mouth, brushing teeth, wearing contact lens, talking on the phone, drinking water, opening pill container, cooking (chopping), cooking (stirring), talking on couch, relaxing on couch, writing on whiteboard, still (standing), working on computer and random*. Each activity was performed by 4 subjects including one left-handed person. They were performed in 5 different environments: bathroom, bedroom, kitchen, living room, and office. It contains activities of cyclic nature such as *brushing teeth* and activities with similar postures such as *drinking water and talking on the phone*.

UTK: There are 10 activities in this dataset: *walk, sit down, stand up, pick up, carry, throw, push, pull, wave hands, and clap hands*. These activities were performed by 10 subjects and repeated twice by each subject. The significant intra-class and viewpoint variations are the main challenges of this dataset.

F3D: This dataset includes 9 activities: *wave, drink from a bottle, answer phone, clap, tight lace, sit down, stand up, read watch, and bow*. These activities were repeated twice or thrice by 10 subjects. The main challenge with this dataset is that the activities were performed at high speed. This provides a small number of frames for the algorithm to sample and learn from.

KARD: This dataset contains 2160 videos and consists of 18 activities. These activities were performed by 10 different people. The 18 activities are *horizontal arm wave, high arm wave, two hand wave, catch cap, high throw, draw X, draw tick, toss paper, forward kick, side kick, take umbrella, bend, hand clap, walk, phone call, drink, sit down, and stand up*. This dataset is challenging due to the large number of activities

with high intra-class variation such as different individuals performing the same activity such as catch cap but in different ways, this makes learning of the same activity with large differences in movements difficult.

MSR: In this dataset there are 16 activities: *drink, eat, read book, call cellphone, write on a paper, use laptop, use vacuum cleaner, cheer up, sit still, toss paper, play game, lie down on sofa, walk, play guitar, stand up, and sit down*. There are 10 subjects, and each subject performed all activities in both standing and sitting positions. This makes the dataset challenging because the extracted features for both sitting and standing positions in each activity are different. Another challenge is data corruption. In some frames, the skeletal gesture structure suddenly collapses completely and lose their coherence and become meaningless.

B. Method

Through preliminary experiments, the best values for swarm size and number of iterations were 20 and 50 respectively. The experiment was repeated 30 times and the average was obtained. The performance of our proposed method (HPGMK) was evaluated by comparing with K-means Clustering (KM), SC, ENSC, SSC [2], and PSO methods. K-means Clustering (KM) and PSO have been chosen for comparison as our proposed HPGMK is based on them. ENSC was found to be most similar to our work as an unsupervised algorithm requiring known cluster number while SSC and SC were the original algorithms that ENSC was based on. To compare the performance of the methods, the accuracy metric (is calculated based on [37]) was used. Moreover, F-score was used to show the performance of each method in categorizing each activity and the confusion between them was shown in confusion matrix. Convergence test and clustering time of HPGMK were measured to evaluate the benefits of each component used in the HPGMK on its performance.

C. Results and discussion

Fig. 8 shows the accuracy of HPGMK with the SOTA techniques for all subjects of each dataset based on the maximum, minimum and average accuracies. The average overall accuracy of the HPGMK was 77.53 % for CAD-60, 56.54 % for UTK, 66.84 % for F3D 46.02 % for KARD and, 40.12 % for MSR. As seen in Fig. 8, HPGMK has the best performance in terms of maximum and average accuracy in all datasets. This shows the effectiveness of the HPGMK for human activity discovery. By utilizing the Gaussian mutation and KM along with PSO, our approach brings performance improvement compared to the other methods. ENSC and SSC, which are subspace clustering algorithms, do not use an efficient search strategy [38]. In these methods, there is no strategy for maintaining the balance between exploitation and exploration in their search. Moreover, Parameters are required to be set and finding the right values for them is tricky and complex such as size of subspace [39]. In contrast, HPGMK are not dependent to parameters like SSC and ENSC and has several strategies for searching. First, it used the PSO to search in large space area by using several particles as

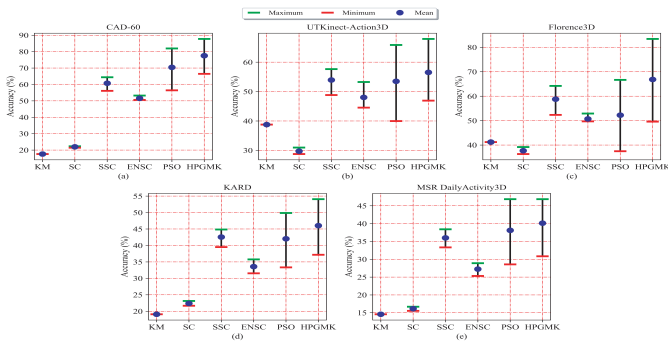


Fig. 8: The average accuracy for all subjects in (a) CAD-60, (b) UTK, and (c) F3D

potential solutions. To promote diversity, Gaussian mutation is used. KM is also used to search in a small area of the global best solution to refine the obtained centroids from PSO. These search strategies, enable HPGMK has a relatively good performance compared to the SSC and ENSC.

Fig. 9(a) to (c) show the effect of each component of each type of the proposed hybrid feature extraction method based on the discovery accuracy of the activities performed by subject one in the CAD-60 dataset. Percentages represent the discovery accuracy using the different combination of features and each piece of graphs shows the ratio of the impact of one component in discovery improvement to the rest of the other components in each type of feature. This ratio is obtained based on dividing *discovery accuracy obtained by one of the components from a feature type* by *summation of discovery accuracy obtained by all components of that feature type*. Overall, in three feature extraction methods comprising displacement, statistical, and orientation features, when all their components are combined, the discovery accuracy significantly increased and obtained 65.45%, 62.54%, and 57.09% respectively. By contrast, if each component of the feature extraction methods is used alone without considering other components in the feature extraction, the accuracy of discovery decreases. Fig. 9(d) shows the effect of different combinations of each of the feature extraction methods. The size of each circle indicates the effectiveness of the features. Based on the obtained results, it is shown that the highest detection accuracy of 85.45% is obtained by combining all the three methods. It indicates that in order to better differentiate between activities, it is necessary to extract features from different aspects of activities. Fig. 10 shows the selected keyframes from walking activity in MSR. As shown, there are a lot of frames with high similarity that by extracting their features, not only do not help to improve discovery but also increase the computational complexity and increase the overlap between other activities because these gestures occur in other activities. However, using local maximum and minimum kinetic energy can find representative frames and reduce complexity. Looking at a window of frames, we can see the selected frames based on the maximum and minimum local energy value. The selected frames show the most differentiation to display the activity sequence. It is worth mentioning that selecting keyframes

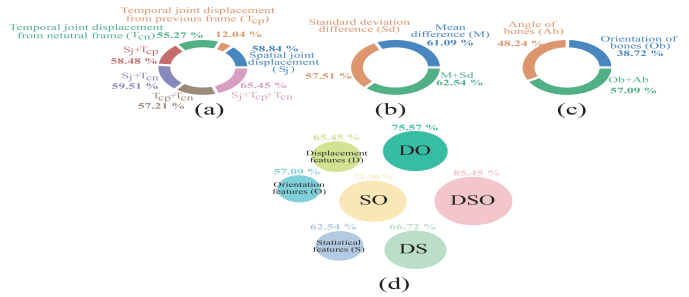


Fig. 9: The effect of the each components of the each type of feature approach including (a) Displacement (D), (b) Statistical (s), and (c) Orientation (O) features, and (d) their various combinations together. Capital letters stand for different methods and putting these letters together means combining relevant methods.

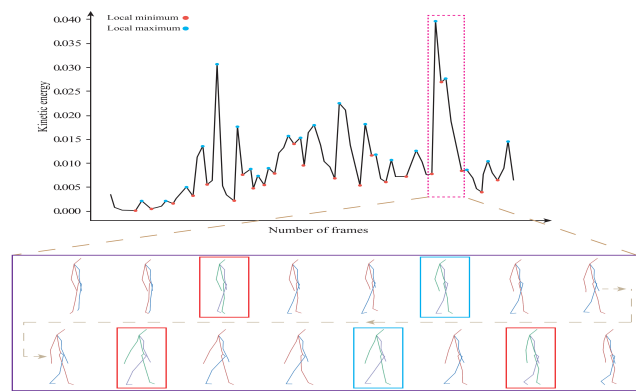


Fig. 10: Illustration of the effect of selecting the keyframe based on kinetic on "walking" in MSR where distinct frames compared to adjacent frames are selected from similar frames. A window of frames is shown with a few selected frames based on the local maximum (blue) and local minimum (red) energy.

maintains the order of the activity.

To show activity discovery performance, confusion matrix in on subject 10 in KARD was shown in Fig. 11 for different methods. This figure demonstrates that HPGMK produced distinctively meaningful clusters. In this figure, cluster overlapping appears relatively high in the other methods especially KM and SC in all datasets. There were a lot of overlapping due to the large number of activities that are very similar including similar body gestures and similar hand movement. For instance, activity overlapping were seen between *High arm wave* and *High throw* with *Drink*.

Fig. 12 shows the average F-score for each activity of all subjects in CAD-60. By examining the average F-scores in most activities, it shows HPGMK outperforming other methods and achieved slightly under 75% on CAD-60 in average for all activities. Although F-score was high in most of the activities for HPGMK compared to other methods, *cooking (chopping)* and *talking on the phone* were discovered with low F-scores. This was due to the high similarity between *cooking (chopping)* with *cooking (stirring)* and *talking on the phone*

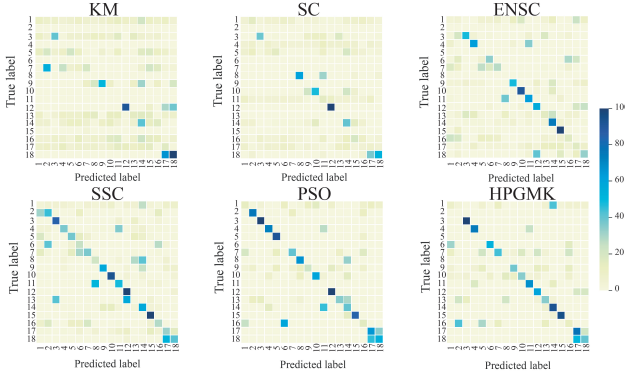


Fig. 11: Comparison of confusion matrix of the result on subject 10 in KARD. Activity list: (1) Horizontal arm wave; (2) High arm wave; (3) Two hand wave; (4) Catch cap; (5) High throw; (6) Draw X; (7) Draw tick; (8) Toss paper; (9) Forward kick; (10) side kick; (11) Take umbrella; (12) Bend; (13) Hand clap; (14) Walk; (15) Phone call; (16) Drink; (17) Sit down; and (18) Stand up.

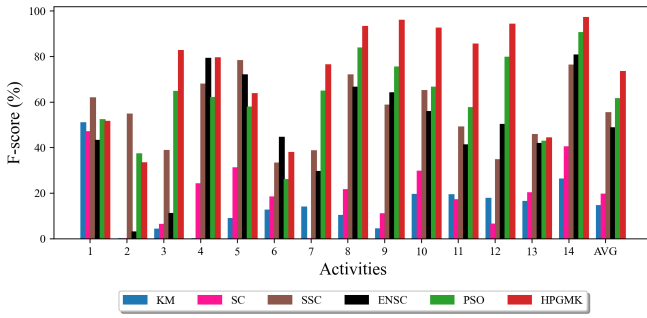


Fig. 12: The average F-score for all subjects in CAD-60. Activity list: (1) Brushing teeth; (2) Cooking (chopping); (3) Rinsing mouth with water; (4) Still(standing); (5) Taking on the couch; (6) Talking on the phone; (7) Wearing contact lenses; (8) Working on computer; (9) Writing on whiteboard; (10) Drinking water; (11) Cooking (stirring); (12) Opening pill container; (13) Random; and (14) Relaxing on couch. AVG is the average F-score for all activities.

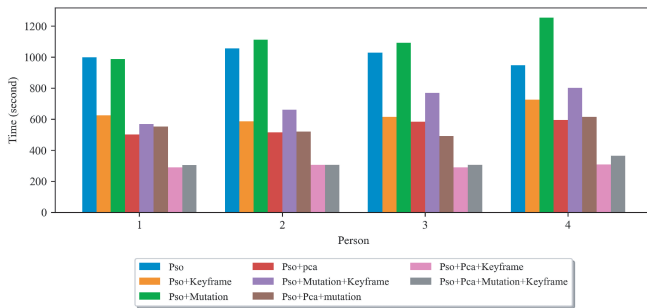


Fig. 13: The comparison of clustering time of different components of proposed algorithm on all subjects in CAD-60 based on (a) without k-means (b) with applying k-means.

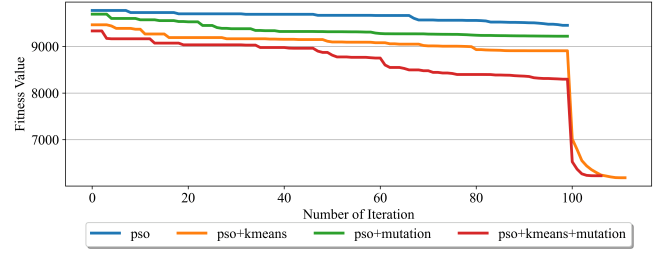


Fig. 14: The comparison of convergence in subject 1 of CAD-60.

with *wearing contact lenses*.

Fig. 13 shows the average clustering time of the different combinations of components used in the proposed algorithm in milliseconds on subject 1 in CAD-60. This experiment evaluates the impact of the different components in the proposed HPGMK algorithm. As can be seen, the clustering time of the proposed algorithm (red line) was relatively low. The reason is that our approach has benefited from dimension reduction methods, including PCA and keyframe selector. Fig. 14 indicates the effect of each component of HPGMK on convergence rate. As it is indicated, each combination has a different convergence rate. However, using all components enables the proposed method to achieve the best convergence compared to the other combinations. It is also confirmed from Fig. 14 that by combining both KM and PSO algorithms, the convergence speed has increased.

V. CONCLUSION

A Hybrid Particle Swarm Optimization with Gaussian Mutation and k-means (HPGMK) approach was proposed to solve human activity discovery on skeleton-based data with no prior knowledge of the label of the activities in the data. Five different datasets were used to assess the performance of the method. The results obtained have shown that HPGMK achieved an average overall accuracy of 77.53 %, 56.54 %, 66.84 %, 46.02 %, and 40.12 % in datasets CAD-60, UTK, F3D, KARD, and MSR, respectively and validate the superiority of HPGMK over other methods compared. In activities with high intra-class variation, corrupted data and the same activity performed in sitting and standing positions, HPGMK has performed better in activity discovery compared to other SOTA methods.

We have examined the impact of each feature used. It was found that the simultaneous combination of features together further improves the results. The impact of the different components in the proposed algorithm have shown that Gaussian mutation has evolved particles to improve search algorithm and k-means has increased the efficiency of discovery and improved the convergence rate.

This work paves the way towards the implementation of fully unsupervised human activity discovery in practical applications using skeleton-based data. There are various factors in the proposed methods that need to be addressed to develop an effective activity discovery algorithm. One factor is the

number of clusters that was pre-configured in the proposed algorithm. The proposed HPGMK need to be further extended to automatically address human activity discovery by estimating the number of activities by itself. Another factor is detecting outlier or noisy data. Outliers shift the cluster centers towards itself, thus affecting optimal cluster formation. It will be beneficial to use outlier detection methods in HPGMK to reject outliers.

ACKNOWLEDGMENT

This work was supported by Grant UBD/RSCH/1.11/FICBF(b)/2019/001 from Universiti Brunei Darussalam.

REFERENCES

- [1] H. V. Chandrashekar *et al.*, "Human activity representation, analysis, and recognition," 2006.
- [2] G. Paoletti, J. Cavazza, C. Beyan, and A. Del Bue, "Subspace clustering for action recognition with covariance representations and temporal pruning," in *2020 25th International Conference on Pattern Recognition (ICPR)*. IEEE, 2021, pp. 6035–6042.
- [3] J. Han, L. Shao, D. Xu, and J. Shotton, "Enhanced computer vision with microsoft kinect sensor: A review," *IEEE transactions on cybernetics*, vol. 43, no. 5, pp. 1318–1334, 2013.
- [4] K. Su, X. Liu, and E. Shlizerman, "Predict & cluster: Unsupervised skeleton based action recognition," in *Proceedings of the IEEE/CVF Conference on Computer Vision and Pattern Recognition*, 2020, pp. 9631–9640.
- [5] J. Shan and S. Akella, "3d human action segmentation and recognition using pose kinetic energy," in *2014 IEEE international workshop on advanced robotics and its social impacts*. IEEE, 2014, pp. 69–75.
- [6] O. M. Nezami, A. Bahrapour, and P. Jamshidlou, "Dynamic diversity enhancement in particle swarm optimization (ddepso) algorithm for preventing from premature convergence," *Procedia Computer Science*, vol. 24, pp. 54–65, 2013.
- [7] B. Jana, S. Mitra, and S. Acharyya, "Repository and mutation based particle swarm optimization (rmppo): A new pso variant applied to reconstruction of gene regulatory network," *Applied Soft Computing*, vol. 74, pp. 330–355, 2019.
- [8] C. Li, S. Yang, and I. Korejo, "An adaptive mutation operator for particle swarm optimization," 2008.
- [9] D. A. Adama, A. Lotfi, C. Langensiepen, K. Lee, and P. Trindade, "Human activity learning for assistive robotics using a classifier ensemble," *Soft Computing*, vol. 22, no. 21, pp. 7027–7039, 2018.
- [10] L. Xia, C.-C. Chen, and J. K. Aggarwal, "View invariant human action recognition using histograms of 3d joints," in *2012 IEEE computer society conference on computer vision and pattern recognition workshops*. IEEE, 2012, pp. 20–27.
- [11] M. Tabejamaat and H. Mohammadzade, "Embedded feature representation in dynamic time warping space for 3d action recognition using kinect depth sensor," *Journal of Machine Vision and Image Processing*, vol. 9, no. 3, pp. 19–34, 2022.
- [12] M. E. Hussein, M. Torki, M. A. Gowayed, and M. El-Saban, "Human action recognition using a temporal hierarchy of covariance descriptors on 3d joint locations," in *Twenty-third international joint conference on artificial intelligence*, 2013.
- [13] J. Sung, C. Ponce, B. Selman, and A. Saxena, "Unstructured human activity detection from rgb-d images," in *2012 IEEE international conference on robotics and automation*. IEEE, 2012, pp. 842–849.
- [14] W. Cao, Y. Lu, and Z. He, "Geometric algebra representation and ensemble action classification method for 3d skeleton orientation data," *IEEE Access*, vol. 7, pp. 132049–132056, 2019.
- [15] X. Liu, Y. Li, and R. Xia, "Rotation-based spatial-temporal feature learning from skeleton sequences for action recognition," *Signal, Image and Video Processing*, vol. 14, no. 6, pp. 1227–1234, 2020.
- [16] M. M. Arzani, M. Fathy, A. A. Azirani, and E. Adeli, "Switching structured prediction for simple and complex human activity recognition," *IEEE transactions on cybernetics*, 2020.
- [17] L. Shi, Y. Zhang, J. Cheng, and H. Lu, "Two-stream adaptive graph convolutional networks for skeleton-based action recognition," in *Proceedings of the IEEE/CVF conference on computer vision and pattern recognition*, 2019, pp. 12026–12035.
- [18] C. Li, C. Xie, B. Zhang, J. Han, X. Zhen, and J. Chen, "Memory attention networks for skeleton-based action recognition," *IEEE Transactions on Neural Networks and Learning Systems*, 2021.
- [19] S. Gaglio, G. L. Re, and M. Morana, "Human activity recognition process using 3-d posture data," *IEEE Transactions on Human-Machine Systems*, vol. 45, no. 5, pp. 586–597, 2014.
- [20] S. K. Yadav, K. Tiwari, H. M. Pandey, and S. A. Akbar, "Skeleton-based human activity recognition using convlstm and guided feature learning," *Soft Computing*, vol. 26, no. 2, pp. 877–890, 2022.
- [21] P. Zhang, C. Lan, W. Zeng, J. Xing, J. Xue, and N. Zheng, "Semantics-guided neural networks for efficient skeleton-based human action recognition," in *Proceedings of the IEEE/CVF Conference on Computer Vision and Pattern Recognition*, 2020, pp. 1112–1121.
- [22] C. Si, W. Chen, W. Wang, L. Wang, and T. Tan, "An attention enhanced graph convolutional lstm network for skeleton-based action recognition," in *proceedings of the IEEE/CVF conference on computer vision and pattern recognition*, 2019, pp. 1227–1236.
- [23] H. Xia and X. Gao, "Multi-scale mixed dense graph convolution network for skeleton-based action recognition," *Ieee Access*, vol. 9, pp. 36475–36484, 2021.
- [24] J. Cai, N. Jiang, X. Han, K. Jia, and J. Lu, "Jolo-gcn: mining joint-centered light-weight information for skeleton-based action recognition," in *Proceedings of the IEEE/CVF Winter Conference on Applications of Computer Vision*, 2021, pp. 2735–2744.
- [25] T. Wang, W. W. Ng, J. Li, Q. Wu, S. Zhang, C. Nugent, and C. Shewell, "A deep clustering via automatic feature embedded learning for human activity recognition," *IEEE Transactions on Circuits and Systems for Video Technology*, 2021.
- [26] M. Liu, Y. Bao, Y. Liang, and F. Meng, "Spatial-temporal asynchronous normalization for unsupervised 3d action representation learning," *IEEE Signal Processing Letters*, 2022.
- [27] P. Gupta, R. McClatchey, and P. Caleb-Solly, "Tracking changes in user activity from unlabelled smart home sensor data using unsupervised learning methods," *Neural Computing and Applications*, vol. 32, no. 16, pp. 12351–12362, 2020.
- [28] W. Qi, H. Su, and A. Aliverti, "A smartphone-based adaptive recognition and real-time monitoring system for human activities," *IEEE Transactions on Human-Machine Systems*, vol. 50, no. 5, pp. 414–423, 2020.
- [29] X. Yan, Y. Ye, X. Qiu, and H. Yu, "Synergetic information bottleneck for joint multi-view and ensemble clustering," *Information Fusion*, vol. 56, pp. 15–27, 2020.
- [30] H. Zhang, W. Zhou, and L. E. Parker, "Fuzzy temporal segmentation and probabilistic recognition of continuous human daily activities," *IEEE Transactions on Human-Machine Systems*, vol. 45, no. 5, pp. 598–611, 2015.
- [31] W.-H. Ong, L. Palafox, and T. Koseki, "Autonomous learning and recognition of human action based on an incremental approach of clustering," *IEEE Transactions on Electronics, Information and Systems*, vol. 135, no. 9, pp. 1136–1141, 2015.
- [32] L. L. Presti and M. La Cascia, "3d skeleton-based human action classification: A survey," *Pattern Recognition*, vol. 53, pp. 130–147, 2016.
- [33] P. Hadikhani and P. Hadikhani, "An adaptive hybrid algorithm for social networks to choose groups with independent members," *Evolutionary Intelligence*, vol. 13, no. 4, pp. 695–703, 2020.
- [34] J. Cai, H. Wei, H. Yang, and X. Zhao, "A novel clustering algorithm based on dpc and pso," *IEEE Access*, vol. 8, pp. 88200–88214, 2020.
- [35] L. Seidenari, V. Varano, S. Berretti, A. Bimbo, and P. Pala, "Recognizing actions from depth cameras as weakly aligned multi-part bag-of-poses," in *Proceedings of the IEEE Conference on Computer Vision and Pattern Recognition Workshops*, 2013, pp. 479–485.
- [36] J. Wang, Z. Liu, Y. Wu, and J. Yuan, "Mining actionlet ensemble for action recognition with depth cameras," in *2012 IEEE Conference on Computer Vision and Pattern Recognition*. IEEE, 2012, pp. 1290–1297.
- [37] B. Peng, J. Lei, H. Fu, L. Shao, and Q. Huang, "A recursive constrained framework for unsupervised video action clustering," *IEEE Transactions on Industrial Informatics*, vol. 16, no. 1, pp. 555–565, 2019.
- [38] Y. Lu, S. Wang, S. Li, and C. Zhou, "Particle swarm optimizer for variable weighting in clustering high-dimensional data," *Machine learning*, vol. 82, no. 1, pp. 43–70, 2011.
- [39] P. Agarwal, S. Mehta, and A. Abraham, "A meta-heuristic density-based subspace clustering algorithm for high-dimensional data," *Soft Computing*, pp. 1–20, 2021.